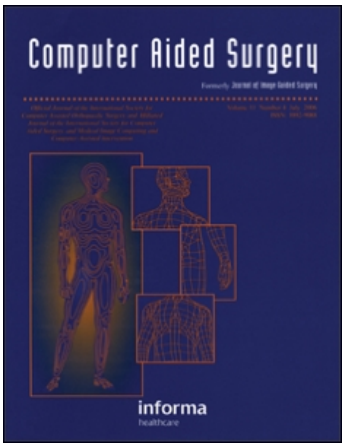

Computer Aided Surgery
Publication details, including instructions for authors and subscription information:
http://www.informaworld.com/smpp/title~content=t713723590

MRI image overlay: Application to arthrography needle insertion

Gregory S. Fischer [a]; Anton Deguet [a]; Csaba Csoma [a]; Russell H. Taylor [a]; Laura Fayad [b]; John A. Carrino [b]; S. James Zinreich [b]; Gabor Fichtinger [ab]
[a] Engineering Research Center, Johns Hopkins University and, Baltimore, Maryland, USA [b] Department of Radiology, Johns Hopkins Hospital, Baltimore, Maryland, USA

Online Publication Date: 01 January 2007

To cite this Article Fischer, Gregory S., Deguet, Anton, Csoma, Csaba, Taylor, Russell H., Fayad, Laura, Carrino, John A., Zinreich, S. James and Fichtinger, Gabor(2007)'MRI image overlay: Application to arthrography needle insertion',Computer Aided Surgery,12:1,2 — 14

To link to this Article: DOI: 10.1080/10929080601169930

URL: http://dx.doi.org/10.1080/10929080601169930

Computer Aided Surgery, January 2007; 12(1): 2–14

informa
healthcare

BIOMEDICAL PAPER

MRI image overlay: Application to arthrography needle insertion

GREGORY S. FISCHER[1], ANTON DEGUET[1], CSABA CSOMA[1], RUSSELL H. TAYLOR[1], LAURA FAYAD[2], JOHN A. CARRINO[3], S. JAMES ZINREICH[2], & GABOR FICHTINGER[1,2]

[1]*Engineering Research Center, Johns Hopkins University and* [2]*Department of Radiology, Johns Hopkins Hospital, Baltimore, Maryland, and* [3]*Department of Radiology, Johns Hopkins Hospital, Baltimore, Maryland, USA*

(Received 30 May 2006; accepted 14 August 2006)

Abstract

Magnetic Resonance Imaging (MRI) offers great potential for planning, guiding, monitoring and controlling interventions. MR arthrography (MRAr) is the imaging gold standard for assessing small ligament and fibrocartilage injury in joints. In contemporary practice, MRAr consists of two consecutive sessions: (1) an interventional session where a needle is driven to the joint space and MR contrast is injected under fluoroscopy or CT guidance; and (2) a diagnostic MRI imaging session to visualize the distribution of contrast inside the joint space and evaluate the condition of the joint. Our approach to MRAr is to eliminate the separate radiologically guided needle insertion and contrast injection procedure by performing those tasks on conventional high-field closed MRI scanners. We propose a 2D augmented reality image overlay device to guide needle insertion procedures. This approach makes diagnostic high-field magnets available for interventions without a complex and expensive engineering entourage. In preclinical trials, needle insertions have been performed in the joints of porcine and human cadavers using MR image overlay guidance; in all cases, insertions successfully reached the joint space on the first attempt.

Introduction and background

Interventional MRI

Magnetic resonance imaging is an excellent imaging modality for the detection and characterization of many human diseases. Its outstanding soft tissue contrast allows for accurate delineation of the pathologic and surrounding normal structures. Thus, MRI has an unmatched potential for guiding, monitoring and controlling therapy [1, 2]. In needle biopsies, the high sensitivity of MRI in detecting lesions allows excellent visualization of the pathology, and the high tissue contrast helps to avoid critical structures in the puncture route [1, 3]. Advances in magnet design and magnetic resonance (MR) system technology, coupled with the development of fast pulse sequences, have contributed to the increasing interest in interventional MRI.

There are a number of technical aspects and concerns to consider when putting an interventional magnet into operation. Among the most pertinent ones are the configuration and field strength of the magnet (which necessitates a compromise between access to the patient and signal-to-noise ratio); the safety and compatibility of the devices and instruments that will be used in or near the magnetic field; the spatial accuracy of imaging for localization and targeting; optimal use of the imaging hardware and software (the dynamic range of gradients, limitation and availability of pulse sequences, radiofrequency coils); and the level of integration with guidance methods for accomplishing the procedure.

Correspondence: Gregory Fischer, 3400 N. Charles St., NEB-B26, Baltimore, MD 21218, USA. Tel: (410)516-3417. Fax: (410)516-3332. E-mail: gfisch@jhu.edu

Part of this research was previously presented at the 14th Annual Medicine Meets Virtual Reality Conference (MMVR14) held in Long Beach, California, in January 2006

ISSN 1092–9088 print/ISSN 1097–0150 online © 2007 Informa UK Ltd.
DOI: 10.1080/10929080601169930

Three main magnet bore configurations are currently used for interventional MRI. The first type, the ''clam shell'' configuration, has a horizontally opened gap and is basically an adaptation and slight modification of the routine open low-field MR unit. The second type, the ''cylinder'' configuration, is an adaptation of a high-field (1.5T or 3.0T) MR unit. Some are made with a flared opening or wider bore to allow an operator to reach in, but in general they do not allow direct patient access for the majority of procedures without robotic or other mechanical assistance. Therefore, imaging and intervention are ''uncoupled''. That is, manipulation of devices or surgical work is done outside the bore, and the patient must then be moved into the magnet for imaging. The third type of configuration is a mid-field (0.5T) magnet specifically designed for intervention, which has two cylinders separated by a gap for access, referred to as the ''double donut'' (SIGNA SP, GE Medical Systems, Milwaukee, WI), but this is no longer offered as a commercial product. A wide variety of procedures may be performed on open magnets, but the trend is to use high-field closed magnets [4], mainly because of the improved imaging quality and wider availability of pulse sequences. The higher the field, the higher the signal-to-noise ratio (SNR). The higher SNR can be used to improve spatial and temporal resolution, and can make techniques like temperature- or flow-sensitive imaging, functional brain MRI, diffusion imaging or MR spectroscopy more useful. Considering these trends, it appears that the use of conventional high-field closed MRI scanners for guidance will allow more successful dissemination of MR-guided techniques to radiology facilities throughout the country and eventually beyond.

We propose using 2D image overlay to guide the needle insertion in procedures where real-time imaging update is not strictly necessary, so that the patient can be translated out of the gantry between imaging and needle insertion. This approach can make diagnostic high-field magnets available for interventions without involving prohibitively complex and expensive engineering additions. Clinical applications highly suited to this technique include musculoskeletal procedures such as arthrography, as well as biopsy and spine injections. MR-guided interventional procedures involving bone, soft tissue, intervertebral discs, and joints are feasible, safe and efficacious. In these applications, clinical success is directly linked to spatial accuracy. Faulty needle placement may also injure sensitive structures, thus subjecting the patient to risk and pain. However, the ultimate effectiveness and adoption of MRI-guided interventions will depend upon the availability of a simple and robust system, similar in complexity to CT- and US-guided interventions.

Limitations of conventional freehand needle placement include the operator's ability to maintain the correct trajectory toward the target, thus causing an increased number of needle passes (iterations). Typically, the guidance images are displayed on the operator's 2D console, on which the intervention is planned. The operator mentally registers the images with the anatomy of the patient, and uses hand-eye coordination to execute the planned intervention. Practitioners generally agree that, given sufficient time and opportunity for intermittent imaging and adjustments, the target can usually be reached with appropriate accuracy. The important question, however, is whether the same objective could be achieved with fewer insertion attempts, because each needle correction requires acquisition of extra images and reinsertion of the needle, thereby increasing the risk of complication, discomfort, and length of the procedure. Hence, the prime objective of our research is to maximize accuracy while minimizing faulty needle insertion attempts under MR guidance.

MRI-guided joint arthrography

Adequately depicting internal derangements of joints has been a challenge for medical imaging. Currently, this evaluation has been improved by the use of MR arthrography (MRAr) [5]. MRAr may be accomplished by way of a percutaneously placed needle approach (referred to as direct MRAr) or with an intravenous injection of a gadolinium-based material (referred to as indirect MRAr). For any joint, the placement of intra-articular contrast (by direct or indirect means) can be used to assist the evaluation of ligaments, cartilage, synovial proliferation or loose intra-articular bodies. MRAr is most commonly used in the shoulder, hip and knee. However, there are also good indications for elbow, wrist and ankle MRAr.

Direct MRAr has become well established as a method of delineating various joint structures that otherwise show poor contrast with conventional MRI. Direct MRAr is well tolerated and has comparable diagnostic efficacy to joint arthroscopy, the gold standard in the evaluation of joints [6, 7]. The main advantages of direct MRAr are the reliable and consistent arthrographic effect and capsular distension produced. However, direct MRAr necessitates image guidance for joint injection, traditionally with fluoroscopy or sometimes under CT guidance [8]. Thus, current direct MRAr comprises two distinct procedures: an initial radiologically guided needle injection intervention

is promptly followed by a second diagnostic MRI session before the contrast becomes resorbed. Such a tightly sequenced double procedure makes contemporary direct MRAr more expensive, resource-intensive, and difficult to schedule. To address this problem, Hilfiker et al. [9] and Ojala et al. [10] reported the use of an open MRI scanner configuration where needle insertion and contrast injection were performed directly inside scanner in the same setting. Lewin et al. [11], and the later Kreitner et al. [12] and Fahrig et al. [13], reported the use of an ''open C-arm scanner'', which consists of a vertically open MRI and optically co-registered C-arm fluoroscope. This approach also eliminated the double scheduling problem by bringing fluoroscopically guided contrast injection and MR-guided joint evaluation into the same room, but at the expense of a complex and expensive engineering entourage, which is neither practical nor generalizable.

Indirect MRAr has emerged as an alternative to direct MR arthrography for imaging joints, in part to obviate the intra-articular needle injection. The main advantage of using indirect MRAr is that there is no need for a fluoroscopy suite. Indirect MRAr may, however, require a longer patient visit because of the time-delay between injection and imaging, which is necessary to provide suitable intra-articular enhancement. Interpretative error may result from the enhancement of extra-articular structures (such as vessels, tendon sheaths and bursae), which may be confounded with extravasated contrast material from the joint [14, 15]. Another limitation of indirect MR arthrography is a lack of controlled joint distension compared with that in direct arthrography [14, 15]. Joint distension facilitates recognition of certain conditions such as capsular trauma or soft tissue injury concealed by a collapsed capsule. Indirect MRAr is often performed when direct arthrography is inconvenient or logistically not feasible.

Thus far, only limited work has been done using MR imaging to guide the needle and contrast placement for MRAr. A cadaver-based study showed that an MR-guided technique in conjunction with the LCD screen and real-time MR imaging would be a practical alternative to conventional fluoroscopic guidance [16]. A case series involving human subjects showed the feasibility of MR-guided MRAr in the shoulder using an open configuration magnet with rapid or real-time imaging [9]. However, with low-field magnets that have a vertically oriented main magnetic field, the traditional radiologic approach to the shoulder must be modified to provide adequate visualization of the needle [11]. MR-guided shoulder MRAr has also been performed on a conventional high-field closed-bore magnet requiring several passes for joint cavity puncture [17]. An extension of this paradigm is to use a robust facile economical targeting system to facilitate joint cavity puncture.

Our approach to direct MRAr is to eliminate the separate radiologically guided needle insertion and contrast injection task from the procedure by performing those tasks directly on a conventional high-field closed MRI scanner using the MR image overlay technique. The hypothesis is that the image overlay technique allows for accurate, safe, and fast needle placement and contrast injection. This promises to reduce the inconvenience for the patient and the logistical difficulties associated with current direct MRAr in a manner that is practical and affordable for any facilities that own conventional MRI scanners.

Surgical assistant techniques

A variety of MR-compatible surgical robots [18–23] have been investigated with a view to assisting image-guided insertions; in every case, the result was a system that is custom-made for one particular application and/or prohibitively complex and expensive for routine clinical use. Numerous types of surgical navigation system (SNS) have been developed to aid the operator by tracking the surgical tool with respect to the imaging device by dynamically referencing fiducials (skin markers, bone screws, a head frame, etc.) attached to the patient's body. Although surgical navigation systems have been commercially available for over a decade, they were not applied in the scanner room except in a handful of limited trials with low-field open MRI [11–13, 24, 25]. While the application of an SNS on high-field closed MRI might seem obvious from certain perspectives, such a transition has not yet been witnessed. The explanation for this can be found in the inherent limitations of a tracked SNS. In theory, the most appealing feature of a tracked SNS is multiplanar image guidance, i.e., when the needle trajectory is shown in three orthogonal images reformatted in real time as the needle moves: the tool is unconstrained while real-time images follow the tool. This works excellently as long as the reformatted images are of good quality, i.e., the image volume is large in all three dimensions and the voxel resolution is uniformly high. Surgical navigation systems also work well on open magnets [24, 25], where the acquisition of MR slices follows the tool in real time. This, however, is not the case with closed-bore magnets, where patients are moved in and out of the bore for needle manipulation. In these procedures, in the interests of saving time,

only a few thin slices are acquired (often only a single image) instead of a thick and dense slab of data. This limitation has a decisive negative impact on the performance of an SNS, because real-time image reformation is now impossible outside the principal plane of imaging (which is typically the transverse plane), thereby depriving the SNS of its best feature. Therefore, the surgical tool (needle) is constrained to a thin image slab or single image. Further problems include the requirement of the optical trackers for an unobstructed line of sight, which may result in a spatial arrangement that disrupts room traffic, and the fact that electromagnetic trackers are incompatible with the MRI room altogether. In short, tracked surgical navigation systems are not well suited to assisting interventions on closed-bore high-field MRI scanners.

In an attempt to fuse imaging information with the operative field, several augmented reality and optical guidance techniques have been investigated. Birkfellner et al. integrated computer graphics into the optical path of a head-mounted stereo binocular [26]. Sauer et al. reported another variant of head-mounted display (HMD) technology [27], in which two head-mounted cameras captured the real scene and a stereo HMD visualized the augmented scene. DiGioia et al. developed a volumetric image overlay system by projecting a 3D virtual image on a semi-transparent mirror in which the physician can simultaneously observe the actual patient and computer-generated images [28, 29]. A similar device using this concept is commercially available under the brand name Dextroscope [30], and this also involves elaborate preoperative calibration and requires real-time spatial tracking of all components, including the patient, physician's head, overlay display, mirror, and surgical tools. Grimson et al. graphically overlaid segmented 3D preoperative images onto video images of the patient [31]. This approach largely posed the same calibration and tracking problems as DiGioia's system, and, in addition, the projected image also had to be warped to conform to the surface of the patient. Iseki et al. created a volumetric overlay display and registered it off-line to the patient in intracranial neurosurgery cases by use of fiducials implanted in the skull [32, 33]. Current volumetric augmented reality devices require painstaking calibration and real-time spatial tracking with the limitations described above, and most current systems depend on complex and expensive hardware.

System implementation

Design

The system concept for the 2D image overlay is shown in Figure 1. A flat-panel display is aligned with a semi-transparent mirror; this unit is mounted in the mouth of an imaging scanner that is able to produce 2D transverse (axial) slices. Typically, the patient is translated out of the bore with the encoded table to position the body under the overlay unit. In short-bore or open scanners, the overlay may be able to coincide with the scan plane. The scanner, display, and mirror are co-aligned so that the reflection of a transverse image appearing in the mirror coincides with the patient's body behind the mirror. The image appears to be floating inside the patient, as if the operator had ''tomographic vision'' by virtually slicing the body. A virtual needle guide is chosen along the specified trajectory, and this guide is superimposed on the overlaid anatomical image. The clinician then inserts the needle using the overlaid guide while

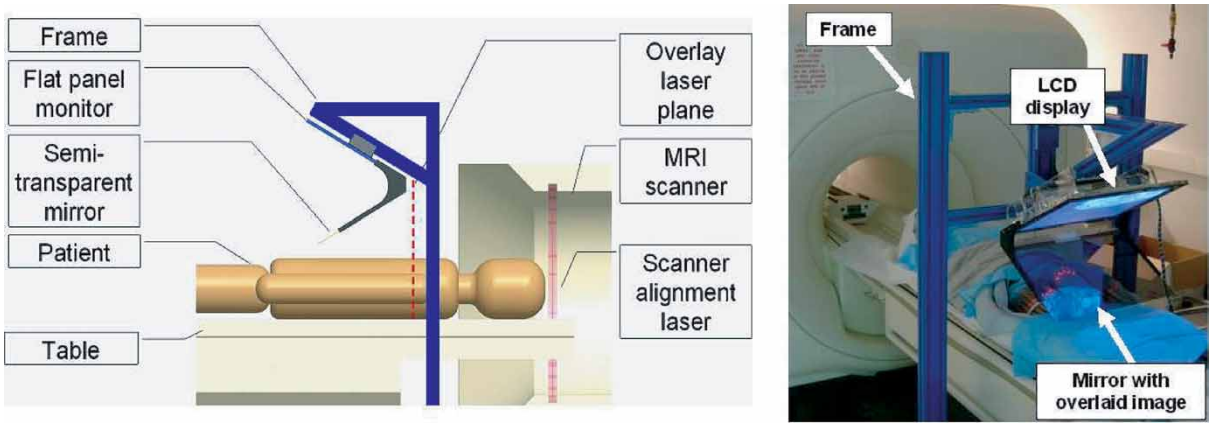

Figure 1. System concept of the 2D image overlay device (left), and the MR image overlay device in a cadaver trial (right). [Color version available online.]

simultaneously being able to see the anatomy and the patient; therefore, his/her focus need never be taken off the patient during the procedure. Our prior work on development of the MR image overlay is described in reference [34].

In earlier work, we investigated CT-guided needle insertion with 2D image overlay, which is similar to the current MR design. A detailed description of the application and analysis of the 2D image overlay technique as applied to CT guidance is described in references [35] and [36]. Also, Stetten et al. have demonstrated a similar 2D overlay technique with applications to ultrasound [37].

As stated earlier, our image overlay system displays transverse MR images on an LCD display, and these are reflected back to the physician from a semi-transparent mirror. Looking through this mirror, the MR image appears to be floating in the correct location in the body. The intersection of the mirror and display surface planes is marked with a transverse laser plane that is used to constrain the needle to the image plane. The current embodiment of the MR overlay system is realized by fixing an MR-compatible LCD screen housed in an acrylic shell to a semi-transparent mirror at a precise angle of 60°. (This angle can be changed, but the critical factor is to match the angle between the LCD and the mirror to that between the mirror and the image plane.) The overlay unit is suspended from a modular extruded fiberglass frame as shown in Figure 1 (right). The freestanding frame arches over the scanner table and allows images to be displayed when the encoded couch is translated out of the bore by a known distance. To maintain the goal of a very practical and low-cost system, an off-the-shelf 19'' LCD display was retrofitted to be MRI-safe and electromagnetically (EM) shielded. The ''home-made'' MR display functions adequately up to 1 meter from the scanner bore on a 1.5T scanner; allowing for sufficient access to the patient by translating the encoded table out, as described in the *Workflow* section below.

To use the system, a small stack of transverse images is acquired and one image is selected as the guidance image. The software flips the image vertically, adjusts its in-plane orientation and magnification, superimposes additional guidance information (e.g., a virtual needle guide, ruler and labels), and renders the modified image on the flat-panel display. Perhaps the most attractive feature of the image overlay system is that the operator has optical guidance in executing the intervention without turning his/her attention away from the field of action, while performing the same actions as in conventional freehand procedures. A close-up view of the overlay system during a procedure is shown in Figure 2. In most needle placement procedures, after the entry point is selected with the use of skin fiducials, the operator must control needle motion with three degrees of freedom (DOF). In this case, the operator uses the overlay image to control the in-plane insertion angle (the first DOF), while holding the needle in the transverse plane marked by a laser light

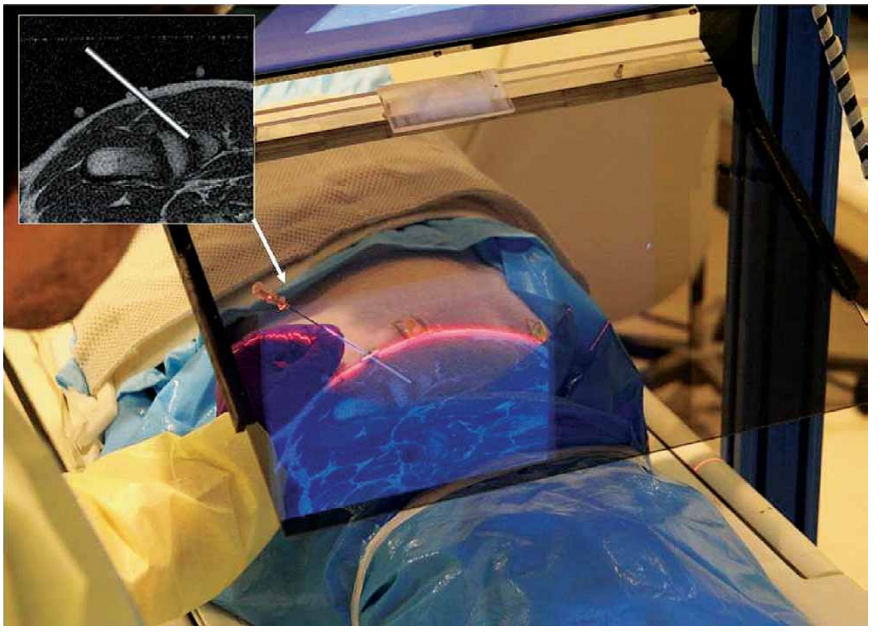

Figure 2. Close-up view of the MR image overlay system in a porcine trial of guiding needle insertions into the joint space of the shoulder. The plan on the targeting image is shown in the inset. [Color version available online.]

(the second DOF). The insertion depth (the third DOF) may be marked with a clamp and/or zebra scale (circumferential marks) on the needle; the overlay display also provides a ruler and depth gauge. The traditional unassisted procedure, to which operators are accustomed, remains unaltered; rather, the amount of visual information in the field of action is increased. As the majority of needle placement procedures are executed ''in plane'' (i.e., when the needle is completely contained in a single image slice), giving up full 3D rendering for engineering simplicity and low cost appears to be a most reasonable trade-off. The overlay image can also help detect target motion and allow gating of the needle insertion by the respiratory cycle. (That is, the needle is advanced forward only when the fiducials on the patient and in the overlay image coincide at the peak of the respiratory cycle.)

In summary, the main advantages of the MR image overlay system as compared to traditional techniques are as follows: (1) The planning image is available for intra-procedural guidance; (2) the physical patient, MR image, needle, and insertion plan are rendered in a single view; (3) optically stable images are provided without auxiliary tracking instrumentation; (4) only visual alignment is required for calibration; (5) the system is inexpensive; and (6) the same view is shared by multiple observers.

Calibration

Calibration is accomplished in three stages: (1) align the overlay image such that it coincides with the plane of the overlay system's laser plane; (2) align the overlay system such that its laser plane is parallel to the transverse imaging plane of the scanner; and (3) determine the in-plane transformation between the overlaid MR image and the view of the physical fiducial marks on the patient in the mirror.

The initial stage of calibration is performed during manufacturing of the device to guarantee that the angle between the laser plane and the mirror and that between the mirror and the LCD are the same in our current prototype. The laser is adjusted such that it passes though the intersection of the LCD and mirror planes while maintaining the correct angle with respect to the mirror (60°). The second stage is performed when the overlay system is brought into the scanner room. To ensure parallelism of the scanner's image plane and the overlaid image, a an arbitrary square box (a common cardboard or plastic box will do) is manually adjusted on the MR table until the scanner's transverse laser plane sweeps the front face of the box; the scanner bed is then translated out and the overlay is positioned such that its onboard laser line generator does the same.

The first step of the in-plane registration stage is image scaling. The overlay image must appear in the correct size in the mirror, but there is variable linear scaling between the MR image and the displayed image. The pixel size of the display is constant and is either known from the manufacturer's specification or can easily be measured. The pixel size of the MR image is extracted from the DICOM header or calculated as the ratio between the field of view (in millimeters) and the image size (in pixels). The second step of in-plane registration is to determine a 3-DOF rigid body transformation. An MR image is acquired of either a calibration phantom or of the patient himself with fiducials placed on the skin, and this image is rendered on the overlay display, as seen in Figure 3. The in-plane rotation and translation of the overlaid image is adjusted until each fiducial marker coincides with its mark in the image. This calibration process is similar to, but significantly simpler than that of the CT image overlay system, which is described in depth in references [35] and [36].

Workflow

In order to increase patient safety and reliability in data reporting, the calibration and system set-up may be verified before each treatment, and

Figure 3. MR image overlay-guided direct MR arthrography in cadaver trials. (a) Targeting image with overlaid guide. (b) Insertion under overlay guidance. (c) Confirmation image with overlaid targeting plan. [Color version available online.]

especially before treating each individual patient. Assuming a pre-procedurally aligned system, the intra-procedural workflow is as follows:

- Place the patient on the table and place the imaging coil over the target site.
- Prepare the site of intervention and place sterile skin fiducials (TargoGrid from Invivo Corp., Orlando, FL) with the parallel bars orthogonal to the approximate slice direction.
- Translate the patient into the scanner and acquire a thin slab of MRI images with appropriate slice thickness for optimal target identification.
- Transfer the image directly in DICOM format to the planning and control software implemented on a stand-alone PC; select the target of interest and the percutaneous puncture point as shown in Figure 3(a).
- Display a visual guide along the trajectory of insertion and render the image on the overlay device.
- Translate out the table with the patient such that the selected entry point is under the gantry's laser plane and mark the plane and/or entry point; continue to translate out the table such that the marked entry point is under the overlay's laser plane.
- Verify the alignment of the overlay image to the patient and, if necessary, update the in-plane alignment as described in the *Calibration* section above.
- Take the needle in hand, reach behind the mirror, touch down on the selected entry point, and rotate the needle to match with the virtual guide while keeping it in the laser plane, as shown in Figure 3(b).
- Verify that the respective fiducials on the patient and in the image coincide; use the skin fiducials to gate or synchronize the needle insertion to the respiratory cycle.
- Insert the needle to the predefined depth while maintaining in-plane and out-of-plane alignment.
- Translate the patient back into the scanner and acquire a confirmation image (Figure 3(c)); if the needle position is satisfactory, perform the rest of the intervention (contrast injection, harvesting of tissue sample, etc.)

Experiments and results

Cadaver trials

The MR overlay system as shown in Figure 1(right) has been successfully tested for compatibility in 1.5T and 3T scanners. Joint arthrography needle insertions have been performed under MR image overlay guidance on porcine and human cadavers in a 1.5T GE Signa scanner using the workflow described earlier. In the porcine cadaver trials, 12 separate insertions were performed in the joint space of the shoulder of three fresh (within one hour of euthanasia in unrelated studies) porcine cadavers. Insertions were performed using 18G, 10-cm MR-compatible needles (EZ-EM, Inc., Lake Success, NY) with insertion depths ranging from 26 to 43 mm. In the human cadaver trials, 10 separate insertions were performed in the joint space of the hip of two cadavers. Again, insertions were performed using 18G, 10-cm MR-compatible needles; insertion depths ranged from 30 to 54 mm. Planning and confirmation images from both sets of trials were examined by two board-certified radiologists to determine whether the tip of the needle landed in the joint space. The needles were successfully inserted into the joint on the first attempt in all cases. An example is shown in Figure 4. Quantitative accuracy analysis was not possible due to the relatively large paramagnetic needle artifact in the MR images and the lack of distinct target points.

To demonstrate the ability to guide percutaneous spinal access, needle insertions have been performed with the MR image overlay on an interventional abdominal phantom (CIRS, Inc., Norfolk, VA). Successful access to all anatomical targets was verified visually with MRI; again, needle artifacts and lack of distinct targets did not allow for precise error measurement. To further verify image overlay capabilities, successful insertions with depths of up to 100 mm have been performed in porcine cadavers. We note that, functionally similar earlier trials with a CT image overlay (where exact target verification and accuracy assessment is possible) have proven the technique to be reliable for guiding percutaneous access on human and porcine cadavers [35, 36].

Comparison of four needle guidance techniques

To further validate the efficacy and accuracy of MR image overlay guidance, four manual needle insertion techniques were compared: (1) image overlay as described above and shown in Figure 5(a); (2) a biplane laser that marks the insertion path with the intersection of two calibrated laser planes, as described in reference [38] and shown in Figure 5(b); (3) a handheld protractor with pre-angled guide sleeve, as shown in Figure 5(c); and (4) conventional unassisted freehand needle insertion. All four techniques involve translating the patient

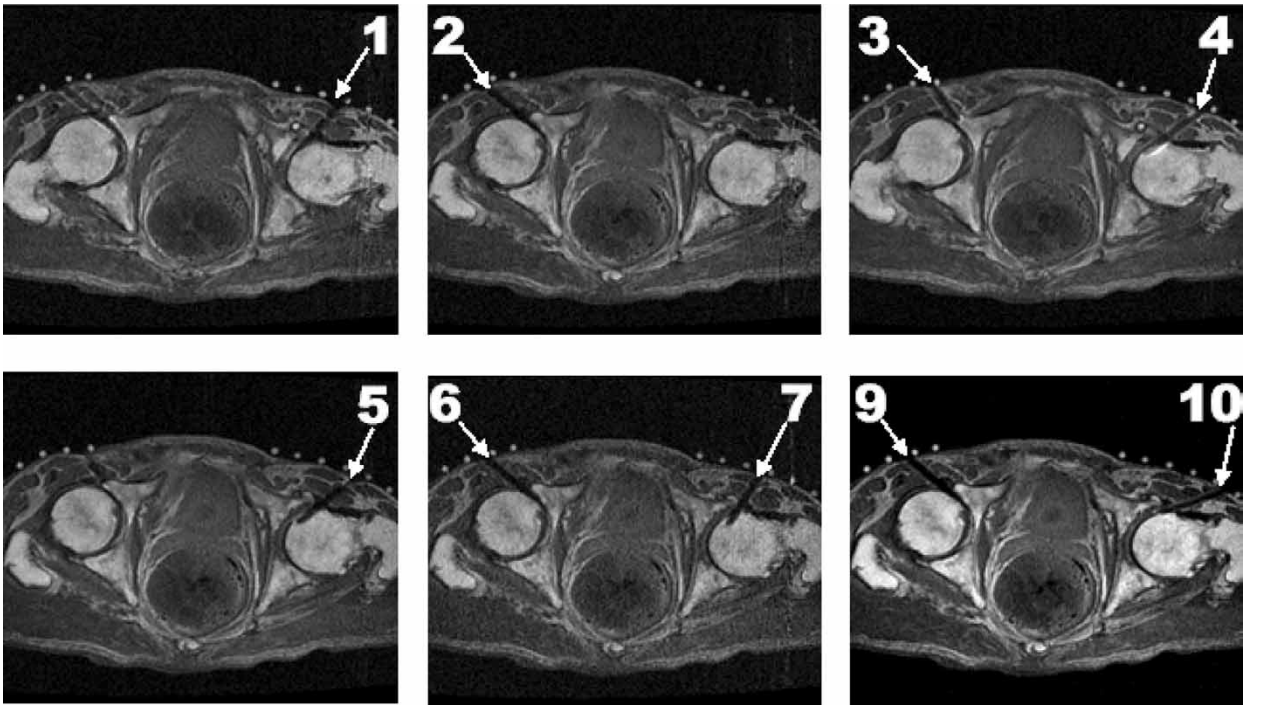

Figure 4. Results from 10 needle insertions into the joint space of the hip of human cadavers under MR image overlay guidance.

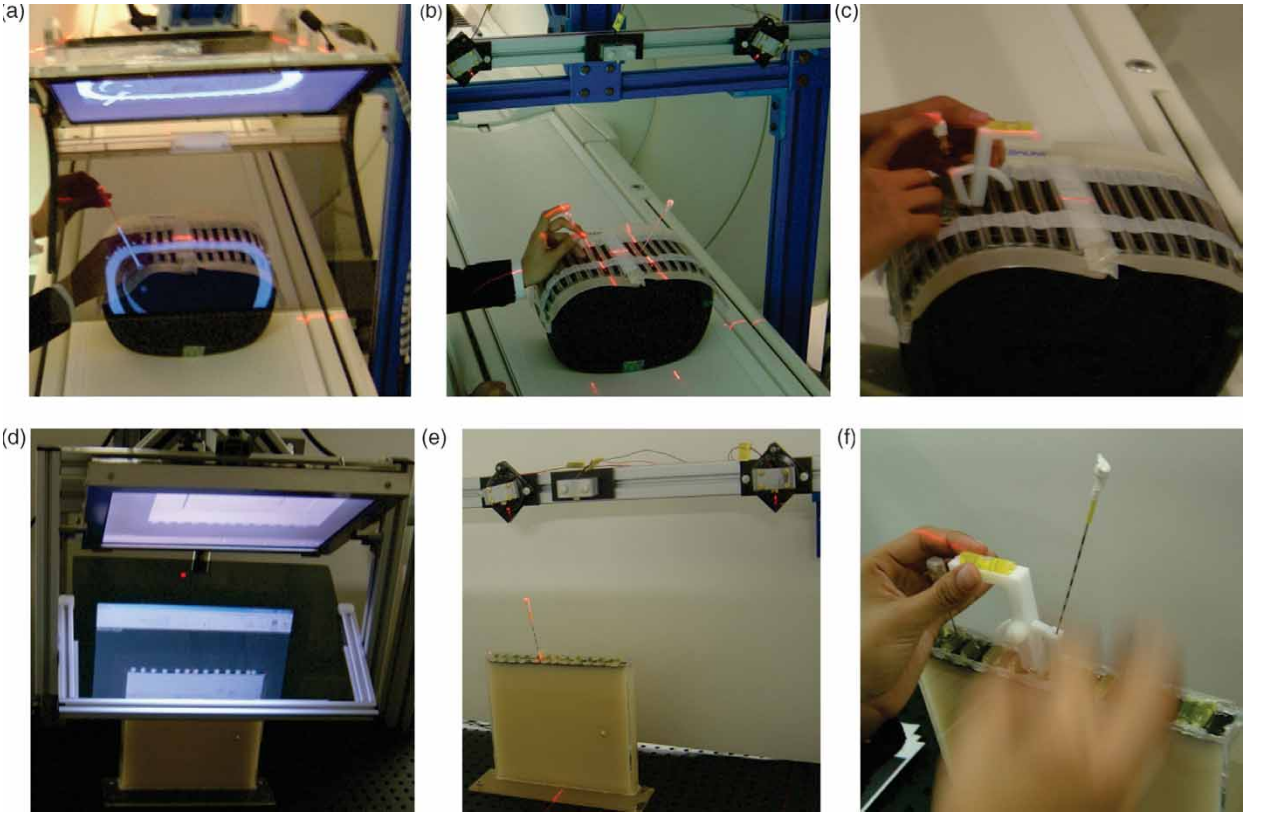

Figure 5. Comparison studies between the MR image overlay (a and d), a biplane laser guide (b and e), a handheld protractor guide (c and f), and the traditional freehand approach. Initial studies were performed under MR imaging (a–c) and follow-up quantitative comparisons were performed in the laboratory with a functionally equivalent system configuration (d–f). [Color version available online.]

out of the scanner for insertion, skin fiducials to determine the puncture point, and manual needle placement in the laser-marked transverse plane. All four are equivalent in controlling out-of-plane angle and depth; therefore, these aspects were not evaluated in these experiments.

Three series of experiments were conducted with a 1.5T GE Signa scanner and 18G MR-compatible beveled needles. The first trial used a CIRS abdominal phantom with TargoGrid fiducials, as shown in Figure 5(a–c); four needle insertions were performed with each technique. In this test, the procedure was performed on the MRI scanner and MRI-based validation was used. All needle insertions with all four techniques appeared to be satisfactory by qualitative visual observation of confirmation MR images, but needle artifacts and the lack of distinct targets rendered quantitative measurement inconclusive. In a similar follow-up trial, four separate needle insertion phantoms were used (one for each technique); these phantoms were of the same type as those in the previous experiment. In this experiment, the same three needle insertions were performed with each technique in the MR scanner, and accuracy measurements were made independently using fluoroscopy, as shown in Figure 6. Although the results are not statistically significant due to the small sample size, the average error between the needle and the target was less than 1 mm for the image overlay, while the other techniques ranged in accuracy from 2 mm to 7 mm (worst being unassisted freehand insertion). These first two experiments serve as a proof of concept for all four techniques in the MR environment.

In the third experiment, we used a phantom filled with two different stiffness layers of tissue-equivalent gel and five embedded 4-mm plastic targets, and covered with neoprene skin. This test was performed based on MR images, but conducted on a functionally equivalent configuration of the devices in a laboratory setting, as shown in Figure 5(d–f). A total of 30 insertions were performed with each technique; C-arm fluoroscopy was used to determine in-plane tip position error and angular error. This experiment serves as a quantitative comparison of the four techniques in the laboratory. Results from this trial are shown in Table 1. Technique made a significant difference in

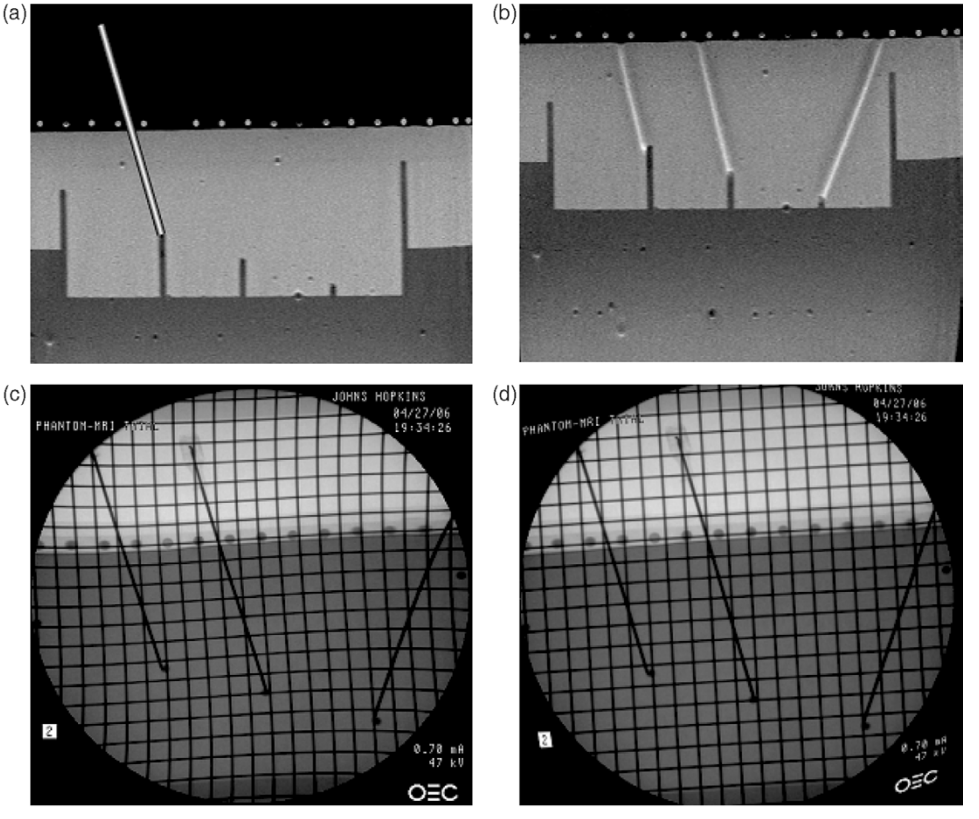

Figure 6. Needle insertion validation procedure for MR image overlay phantom trials using fluoroscopy. (a) A plan is generated and displayed on the overlay. (b) The needle is inserted and a confirmation MR image acquired. (c) The phantom is placed in a C-arm fluoroscope and a fluoroscopic image is acquired. (d) Measurements are made on a dewarped version of the fluoroscopic image.

Table 1. Results from a quantitative comparison between the three assisted techniques and the traditional freehand technique in the equivalent laboratory system configuration. In-plane needle insertion accuracy is presented for the four techniques with 30 insertions each.

Technique	Avg. position error (mm)	Std. dev. position err.	Avg. orientation error (deg)	Std. dev. orientation err.
Freehand	5.27	5.56	4.07	4.11
Protractor	5.37	7.36	3.35	3.34
Laser	2.90	2.62	2.02	2.22
Overlay	2.00	1.70	2.41	2.27

tip position error ($p = 0.015$) and angle error ($p = 0.053$). With a 75% confidence interval, biplane laser and image overlay provide for better tip placement accuracy than the other techniques. With an 80% confidence interval, biplane laser and image overlay have better angular accuracy than the other techniques. In terms of angular and positional accuracies, no significant difference was found between the laser guide and image overlay in these preliminary studies.

Discussion

Initial cadaver and phantom experiments support the hypothesis that the MR image overlay can provide accurate needle placement while significantly simplifying the arthrography procedure by eliminating separate radiographically guided contrast injection. The system also appears to be useful in spinal and other musculoskeletal needle placement procedures; however, independent measurement of accuracy will have to support this claim in later trials. In our studies, by visualizing target anatomy and providing a visual guide, the MR image overlay consistently allowed accurate needle placement on the first attempt.

There were many lessons learned and hurdles overcome in the development of this system. The first hurdle was transitioning the CT-compatible system to MRI, which required ensuring MR-compatibility of the flat-panel display. The current display is a standard LCD display that had the steel casing replaced with aluminum EM shielding. The display can function adequately at distances up to 1 meter from the scanner bore before saturation of the ferrite core inductors occurs; we are investigating options that will allow the overlay unit to be moved in closer to the scanner. Another issue that arises with 2D image overlay in general is parallax, as described in reference [35]; the key is to minimize the parallax error by decreasing the thickness of the mirror, while maintaining rigidity of the mirror to prevent sagging. We have settled on 4-mm-thick smoked acrylic sheets as the semi-transparent mirror material. Visibility of the overlaid image in the mirror is dependent on the room lighting; we have found that dimming the lights enhances the overlaid image, but in turn decreases the visibility of the patient and the needle behind the mirror. Typically, lights behind the clinician are dimmed while maintaining illumination on the opposite side; the optimal configuration appears to be based on the clinician's preference. Calibration of the device is an aspect that has evolved significantly from our early experiments with 2D image overlay. We used to believe that a full calibration for in-plane alignment was necessary during set-up of the system. The procedure has since evolved into simply aligning the image in the overlay with the skin fiducials on the patient; this is faster and simpler to perform, and also safer since it guarantees alignment of the guide with the patient at the time of insertion. Further, this eliminates the need for a special calibration phantom for alignment with the patient, as described in the *Calibration* section; any object with a flat vertical face can be used to ensure parallelism between the system and the scanner during system set-up.

During the experiments, it was revealed that holding the needle in the plane of insertion can be difficult, especially for non-expert users. We attempted to ease this problem with a mechanical needle guide – a horizontal bar attached to the display-mirror unit, as shown in Figure 7(a). The bar is made of acrylic and its height is adjustable. The operator places the needle at the skin entry-point and presses the needle gently against the bar while inserting the needle. Although not yet implemented, a stronger constraint can be provided by adding a sliding-rotating needle guide with a quick-release mechanism, as shown in Figure 7(b). Although mechanical constraints are redundant in addition to optical guidance, they appear to be very useful for increasing the level of comfort and confidence of some operators. Preliminary results suggested that as the user becomes more accustomed to the image overlay device, the benefits of mechanical

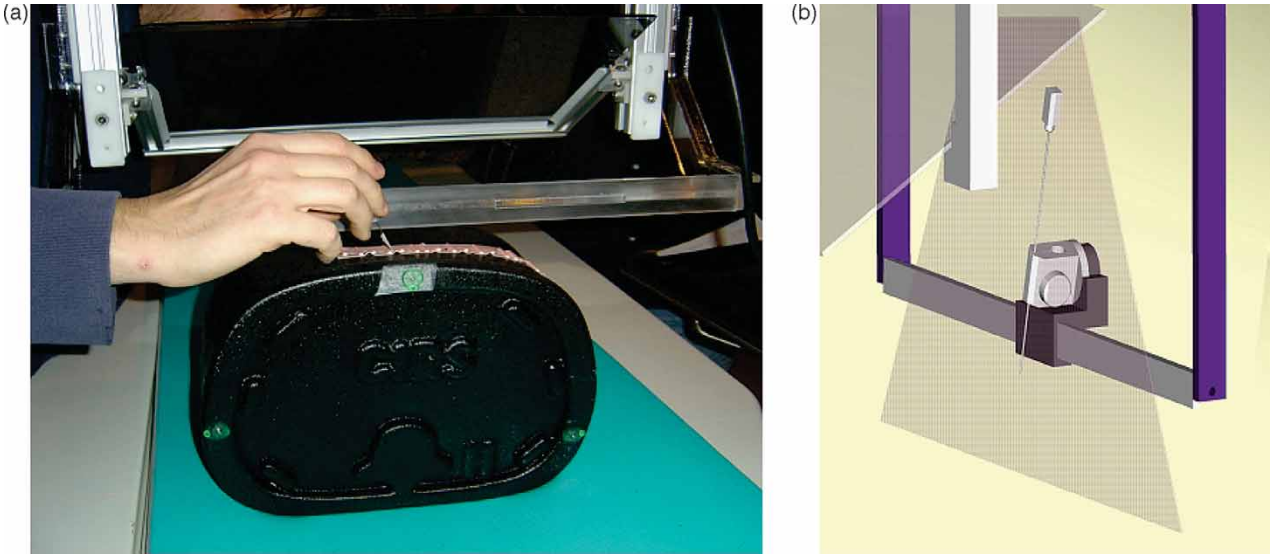

Figure 7. Mechanical needle guide for maintaining the needle orientation in the image plane (shown with the CIRS abdominal phantom). (b) Design of an adjustable angle needle guide to maintain both in-plane and out-of-plane orientation. [Color version available online.]

constraints diminished and can, in fact, become a hindrance. IRB approval has recently been granted for large-scale trials with phantoms to determine the optimal combination of visual and mechanical assistance. We will conduct extensive operator motion and performance analysis, as well as human-machine interface ergonomics studies. IRB approval was required because the ''human subjects'' in these studies will be the operators.

From the comparison studies, enhanced needle insertion techniques appear to provide substantial benefits compared to conventional needle insertion. In the relatively straightforward phantom experiment, biplane laser and image overlay guidance performed similarly. For cases where it is unnecessary to see the target anatomy, the biplane laser appears to be adequate. However, when visualization of the target anatomy is preferred, such as when performing needle placement in the joints or other musculoskeletal targets, the image overlay appears to offer significant advantages over other techniques.

Presently, IRB approval is being sought to commence clinical trials for MR image overlay-guided joint arthrography.

The current overlay system is limited to the transverse plane. Concurrently, a dynamic overlay system is under development, which will be smaller in size and moved over the body to allow needle insertion in arbitrary tilted planes, thereby significantly increasing the flexibility and user-friendliness of the system.

Acknowledgments

The authors would like to acknowledge Iulian Iordachita for assistance in manufacturing the overlay device, Daniel Schlattman for help with shielding the LCD display for MR compatibility, and Hugh Wall for help with operating the scanner. Partial funding for this project was provided by NSF Engineering Research Center Grant #EEC-97-31478, Siemens Corporate Research, and the William R. Kenan, Jr. Fund.

References

1. Jolesz FA. Interventional and intraoperative MRI: A general overview of the field. J Magn Reson Imaging 1998;8(1):3–7.
2. Jolesz FA, Talos IF, Schwartz RB, Mamata H, Kacher DF, Hynynen K, McDannold M, Saivironporn P, Zao L. Intraoperative magnetic resonance imaging and magnetic resonance imaging-guided therapy for brain tumors. Neuroimaging Clin N Am 2002;12(4):665–683.
3. Lenchik L, Dovgan DJ, Kier R. CT of the iliopsoas compartment: Value in differentiating tumor, abscess, and hematoma. Am J Roentgenol 1994;162:83–86.
4. Salomonowitz E. MR imaging-guided biopsy and therapeutic intervention in a closed-configuration magnet: Single-center series of 361 punctures. Am J Roentgenol 2001;177(1): 159–163.
5. Steinbach LS, Palmer WE, Schweitzer ME. Special focus session: MR arthrography. Radiographics 2002;22(5): 1223–1246.
6. Schmitt R, Christopoulos G, Meier R, Coblenz G, Frohner S, Lanz U, Krimmer H. Direct MR arthrography of the wrist in comparison with arthroscopy: A prospective study on 125 patients. Rofo 2003;175(7):911–1019.

7. Schulte-Altedorneburg G, Gebhard M, Wohlgemuth WA, Fischer W, Zentner J, Wegener R, Balzer T, Bohndorf K. MR arthrography: Pharmacology, efficacy and safety in clinical trials. Skeletal Radiol 2003;32:1–12.
8. Binkert CA, Verdun FR, Zanetti M, Pfirrmann CW, Hodler J. CT arthrography of the glenohumeral joint: CT fluoroscopy versus conventional CT and fluoroscopy – comparison of image-guidance techniques. Radiology 2003; 229(1):153–158.
9. Hilfiker PR, Weishaupt D, Schmid M, Dubno B, Hodler J, Debatin JF. Real-time MR-guided joint puncture and arthrography. Eur Radiol 1999;9(2):201–204.
10. Ojala R, Klemola R, Karppinen J, Sequeiros RB, Tervonen O. Sacro-iliac joint arthrography in low back pain: Feasibility of MRI guidance. Eur J Radiol 2001;40(3): 236–239.
11. Petersilge CA, Lewin JS, Duerk JL, Hatem SF. MR arthrography of the shoulder: Rethinking traditional imaging procedures to meet the technical requirements of MR imaging guidance. AJR Am J Roentgenol 1997;169(5):1453–1457.
12. Kreitner KF, Loew R, Runkel M, Zollner J, Thelen M. Low-field MR arthrography of the shoulder joint: Technique, indications, and clinical results. Eur Radiol 2003;13(2):320–329.
13. Fahrig R, Butts K, Rowlands JA, Saunders R, Stanton J, Stevens GM, Daniel BL, Wen Z, Ergun DL, Pelc NJ. A truly hybrid interventional MR/X-ray system: Feasibility demonstration. J Magn Reson Imaging 2001;13(2):294–300.
14. Zoga AC, Schweitzer ME. Indirect magnetic resonance arthrography: Applications in sports imaging. Top Magn Reson Imaging 2003;14(1):25–33.
15. Bergin D, Schweitzer ME. Indirect magnetic resonance arthrography. Skeletal Radiol 2003;32(10):551–558.
16. Trattnig S, Breitenseher M, Pretterklieber M, Kontaxis G, Rand T, Helbich T, Imhof H. MR-guided joint puncture and real-time MR-assisted contrast media application. Acta Radiol 1997;38(6):1047–1049.
17. Trattnig S, Breitenseher M, Rand T, Bassalamah A, Schick S, Imhof H, Petersilge CA. MR imaging-guided MR arthrography of the shoulder: Clinical experience on a conventional closed high-field system. AJR Am J Roentgenol 1999;172(6):1572–1574.
18. DiMaio S, Fischer G, Haker S, Hata N, Iordachita I, Tempany C, Fichtinger G. Design of an prostate needle placement robot in MRI scanner. In: Proceedings of IEEE International Conference on Biomedical Robotics, Pisa, Italy, February 2006.
19. Krieger A, Susil RC, Menard C, Coleman JA, Fichtinger G, Atalar E, Whitcomb LL. Design of a novel MRI compatible manipulator for image guided prostate intervention. IEEE Trans Biomed Eng 2005;52(2):306–313.
20. Hata N, Hashimoto R, Tokuda J, Morikawa S. Needle guiding robot for MR-guided microwave thermotherapy of liver tumor using motorized remote-center-of-motion constraint. In: Proceedings of the 5th Interventional MRI Symposium, Boston, MA, October 2004.
21. Bock M, Zimmermann H, Gutmann B, Melzer A, Fischer H, Semmler W. Combination of a fully MR-compatible robotical assistance system for closed-bore high-field MRI scanners with active device tracking and automated image slice positioning. In: Proceedings of the Radiological Society of North America (RSNA 2004), Chicago, IL, 28 November–3 December 2004.
22. Chinzei K, Miller K. Towards MRI guided surgical manipulator. Med Sci Monit 2001;7(1):153–63.
23. Masamune K, Inagaki T, Takai N, Suzuki M. MRI compatible needle insertion manipulator and image distortion measurement for the evaluation. J JSCAS 2001;3(4):273–280.
24. Lewin JS, Petersilge CA, Hatem SF, Duerk JL, Lenz G, Clampitt ME, Williams ML, Kaczyinski KR, Lanzieri CF, Wise AL, Haaga JR. Interactive MR imaging-guided biopsy and aspiration with a modified clinical C-arm system. Am J Roentgenol 1998;170:1593–1601.
25. Lewin JS, Nour SG, Duerk JL. Magnetic resonance image-guided biopsy and aspiration. Top Magn Reson Imaging 2000;11(3):173–183.
26. Birkfellner H, Figl W, Huber K, Watzinger F, Wanschitz F, Hummel J, Hanel R, Greimel W, Homolka P, Ewers R, Bergmann H. A head-mounted operating binocular for augmented reality visualization in medicine – design and initial evaluation. IEEE Trans Med Imag 2002;21(8): 991–997.
27. Sauer F, Khamene A, Vogt S. An augmented reality navigation system with a single-camera tracker: System design and needle biopsy phantom trial. In: Dohi T, Kikinis R, editors. Proceedings of the 5th International Conference on Medical Image Computing and Computer-Assisted Intervention (MICCAI 2002), Tokyo, Japan, September 2002. Part II. Lecture Notes in Computer Science 2489. Berlin: Springer; 2002. pp 116–124.
28. Blackwell M, Nikou C, DiGioia AM, Kanade T. An image overlay system for medical data visualization. In: Wells WM, Colchester A, Delp S, editors. Proceedings of the 1st International Conference on Medical Image Computing and Computer-Assisted Intervention (MICCAI'98), Cambridge, MA, October 1998. Lecture Notes in Computer Science 1496. pp 232–240.
29. DiGioia AM, Colgan BD, Koerbel N. Computer aided surgery. In: Satava RM, editor. Cybersurgery: Advanced Technologies for Surgical Practice. New York: John Wiley & Sons; 1998. pp 121–139.
30. Kockro RA, Serra L, Tseng-Tsai Y, Chan C, Yih-Yian S, Gim-Guan C, Lee E, Hoe LY, Hern N, Nowinski WL. Planning and simulation of neurosurgery in a virtual reality environment. Neurosurgery 2000;46(1):118–135.
31. Grimson WEL, Ettinger GJ, White SJ, Lozano-Perez L, Wells WM III, Kikinis R. An automatic registration method for frameless stereotaxy, image guided surgery, and enhanced reality visualization. IEEE Trans Med Imag 1996;15(2): 129–139.
32. Iseki H, Masutani Y, Iwahara M, Tanikawa T, Muragaki Y, Taira T, Dohi T, TakaKura K. Volumegraph (overlaid three-dimensional image-guided navigation), clinical application of augmented reality in neurosurgery. Stereotact Funct Neurosurg 1997;68:18–24.
33. Nakajima S, Nakamura K, Masamune K, Sakuma I, Dohi T. Three-dimensional medical imaging display with computer-generated integral photography. Computer Med Imag Graph 2001;25:235–241.
34. Fischer GS, Deguet A, Schlattman D, Taylor RH, Fayad L, Zinreich SJ, Fichtinger G. MRI image overlay: Applications to arthrography needle insertion. In: Proceedings of the 14th Annual Medicine Meets Virtual Reality Conference (MMVR14), Long Beach, CA, January 2006. Amsterdam: IOS Press; 2006. pp. 150–155.
35. Fichtinger G, Deguet A, Masamune K, Fischer GS, Balogh E, Mathieu H, Taylor RH, Zinreich SJ, Fayad LM. Image overlay guidance for needle insertions in CT scanner. IEEE Trans Biomed Eng 2005;52: 1415–1424.

36. Fichtinger G, Deguet A, Fischer GS, Balogh E, Masamune K, Taylor RH, Fayad LM, Zinreich SJ. CT image overlay for percutaneous needle insertions. Comput Aided Surg 2005;10(4):241–255.
37. Stetten GD, Chib VS. Overlaying ultrasonographic images on direct vision. J Ultrasound Med 2001;20(3):235–240.
38. Fischer GS, Wamsley C, Zinreich SJ, Fichtinger G. Laser-assisted MRI-guided needle insertion and comparison of techniques. In: Proceedings of the 6th Annual Conference of the International Society for Computer Assisted Orthopaedic Surgery (CAOS-International 2006), Montreal, Canada, June 2006.